SUPPLEMENTARY INFORMATION

Kcnn4 is a regulator of macrophage multinucleation in bone homeostasis and inflammatory disease

Heeseog Kang[1*], Audrey Kerloc'h[2*], Maxime Rotival[3*], Xiaoqing Xu[1*], Qing Zhang[1*], Zelpha D'Souza[4], Michael Kim[1], Jodi Carlson Scholz[5], Jeong-Hun Ko[2], Prashant K Srivastava[3], Jonathan R. Genzen[6], Weiguo Cui[7], Timothy J Aitman[4], Laurence Game[8], James E Melvin[9], Adedayo Hanidu[10], Janice Dimock[10], Jie Zheng[10], Donald Souza[10], Aruna K Behera[10], Gerald Nabozny[10], H. Terence Cook[2], J H Duncan Bassett[11], Graham R Williams[11], Jun Li[10], Agnès Vignery[1¶], Enrico Petretto[3¶] and Jacques Behmoaras[2¶]

[1]Yale University School of Medicine, Departments of Orthopaedics and Cell Biology, New Haven, CT 06510, USA

[2]Centre for Complement and Inflammation Research (CCIR), Imperial College London, W12 0NN, UK

[3]Integrative Genomics and Medicine, MRC Clinical Sciences Centre, Imperial College London, W12 0NN, UK

[4]Physiological Genomics and Medicine, MRC Clinical Sciences Centre, Imperial College London, W12 0NN, UK

[5]Section of Comparative Medicine, Yale School of Medicine, 310 Cedar Street, New Haven, CT 06510, USA

[6]Department of Pathology, University of Utah and ARUP Laboratories, Salt Lake City, UT 84108

[7]Blood Center of Wisconsin, 8727 Watertown Plank Road, Milwaukee, WI, 53213

[8]Genomics Laboratory, MRC Clinical Sciences Centre, Imperial College London, W12 0NN, London, UK

[9]National Institute of Dental and Craniofacial Research (NIDCR), National Institute of Health, Bethesda, MD 20892, USA

[10]Department of Immunology and Inflammation, Boehringer Ingelheim Pharmaceuticals, Inc., Ridgefield, CT 06877, USA

[11]Molecular Endocrinology Group, Department of Medicine, Imperial College London, W12 0NN, UK

*Co-first authors listed alphabetically

[¶]Corresponding authors

Correspondence should be addressed to Jacques Behmoaras (Jacquesb@imperial.ac.uk); or Enrico Petretto (enrico.petretto@imperial.ac.uk); or Agnès Vignery (agnes.vignery@yale.edu).

Figure S1. Related to Figure 1. WKY macrophages fuse spontaneously to form multinucleated giant cells *in vitro* and during crescentic glomerulonephritis. (**A**) BMDMs from NTN-susceptible WKY and NTN-resistant LEW rats were cultured and cells were fixed at different time points (Day 2 to Day 6). Total RNA was extracted at Day 2, Day 4 and Day 6 to assess *Mmp-9* expression as readout of macrophage giant cell formation by qRT-PCR. Original bars = 25 µm (**B**) Actin cytoskeleton (phalloidin) in spontaneously formed multinucleated giant cells in WKY BMDMs (nuclei staining: DAPI, original bars = 50 µm). (**C**) CD68 (ED-1) staining of a WKY glomerulus showing multinucleated ED1+ giant cells following the induction of NTN (day 10); original bars = 25 µm. Error bars indicate SEM.

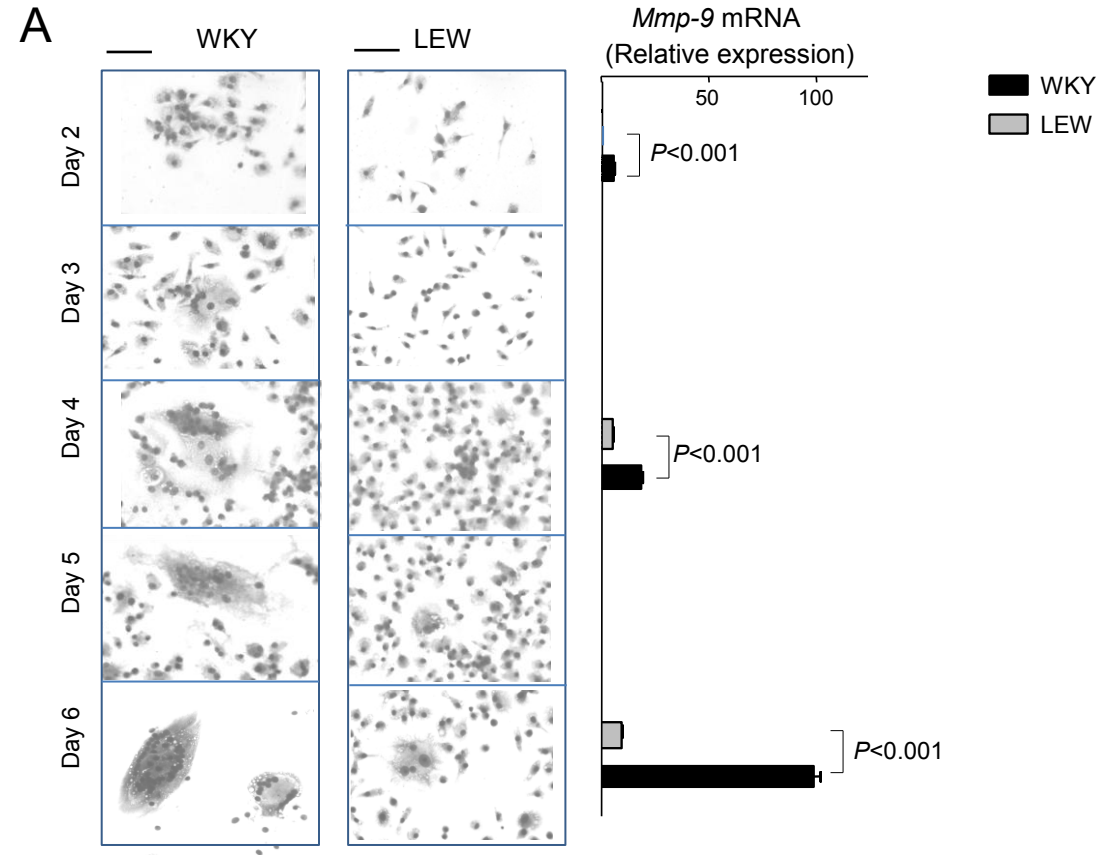

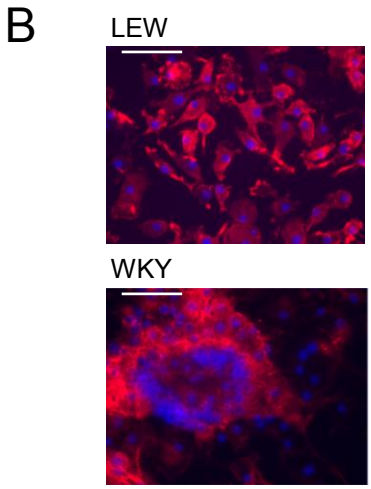

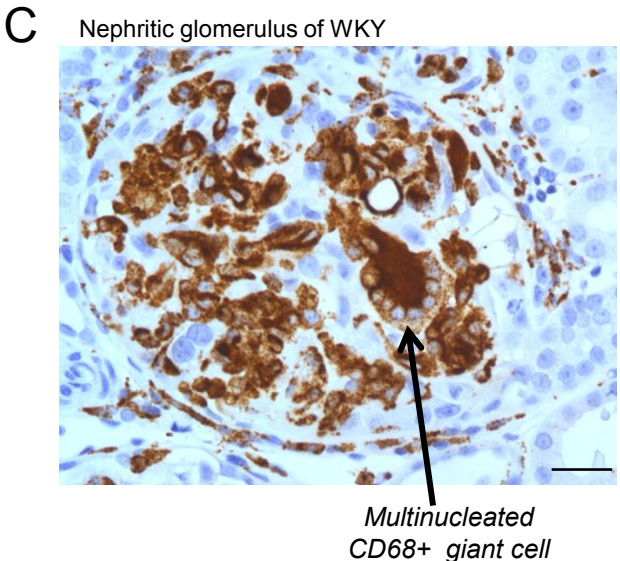

Figure S2

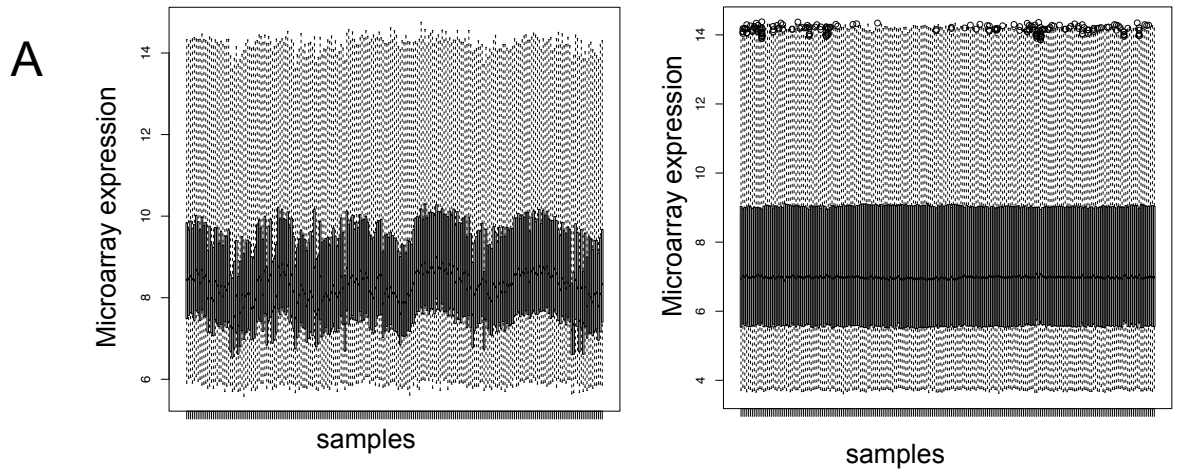
A
Microarray expression
samples
Microarray expression
samples

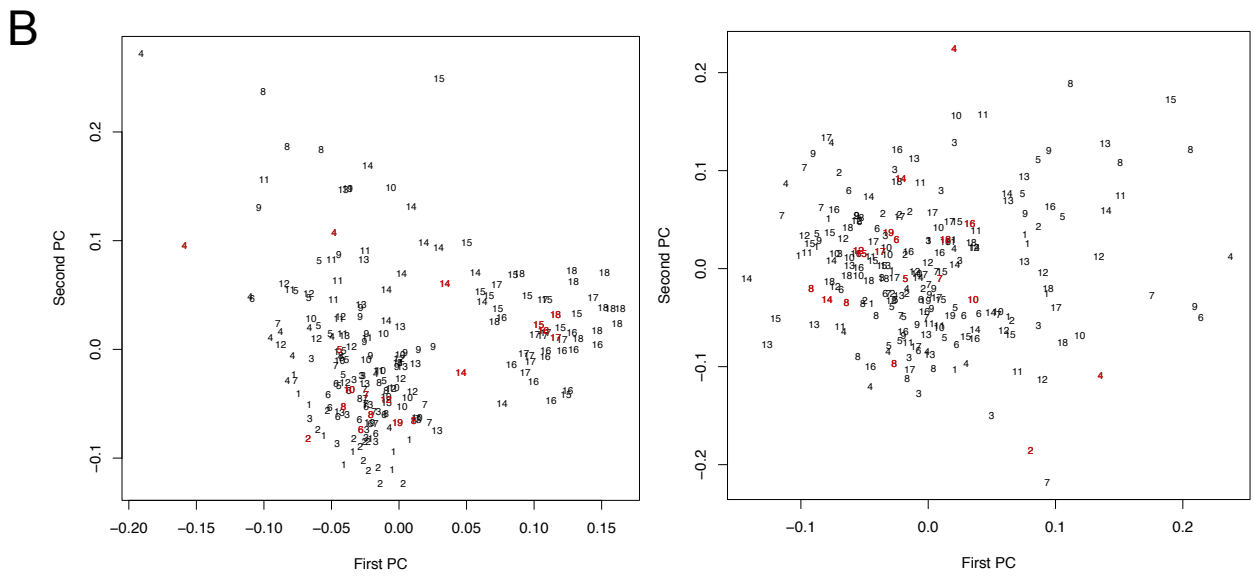
B
Second PC
First PC
Second PC
First PC

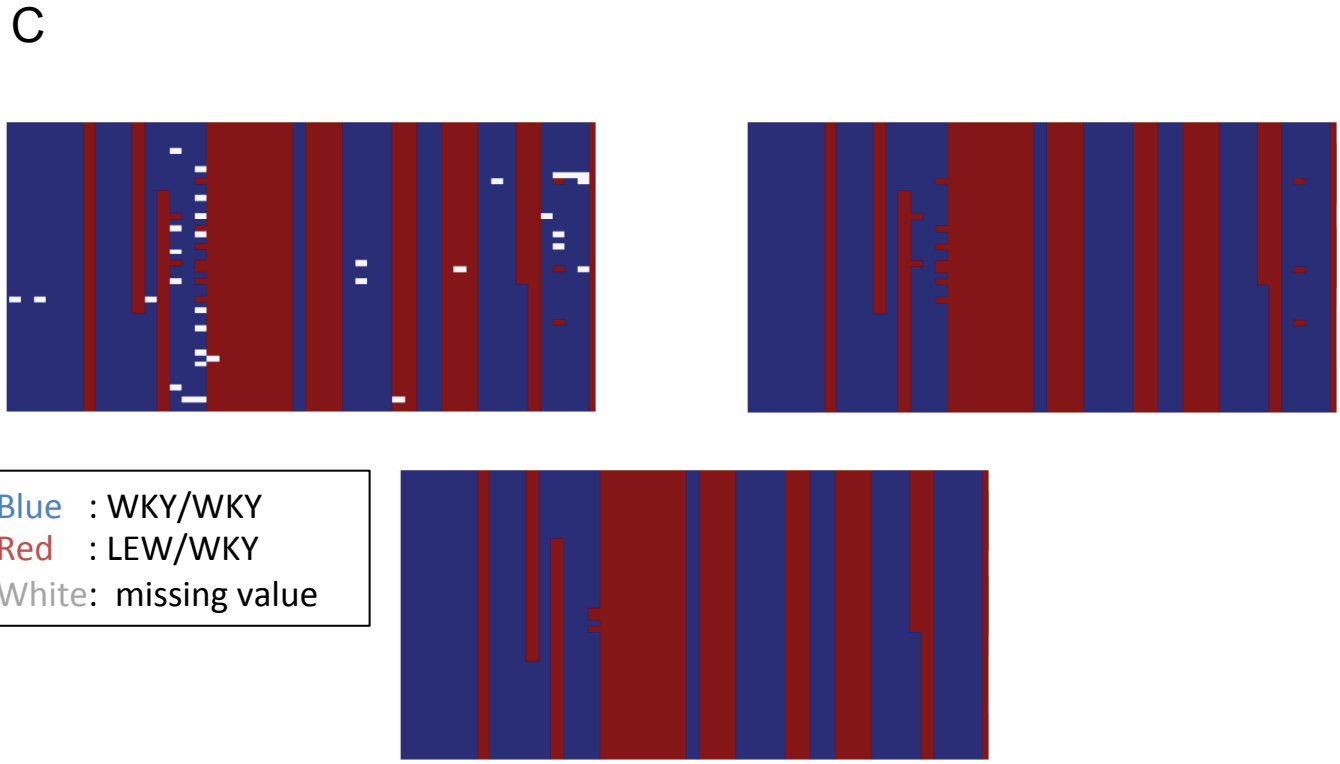
C
Blue : WKY/WKY
Red : LEW/WKY
White: missing value

D

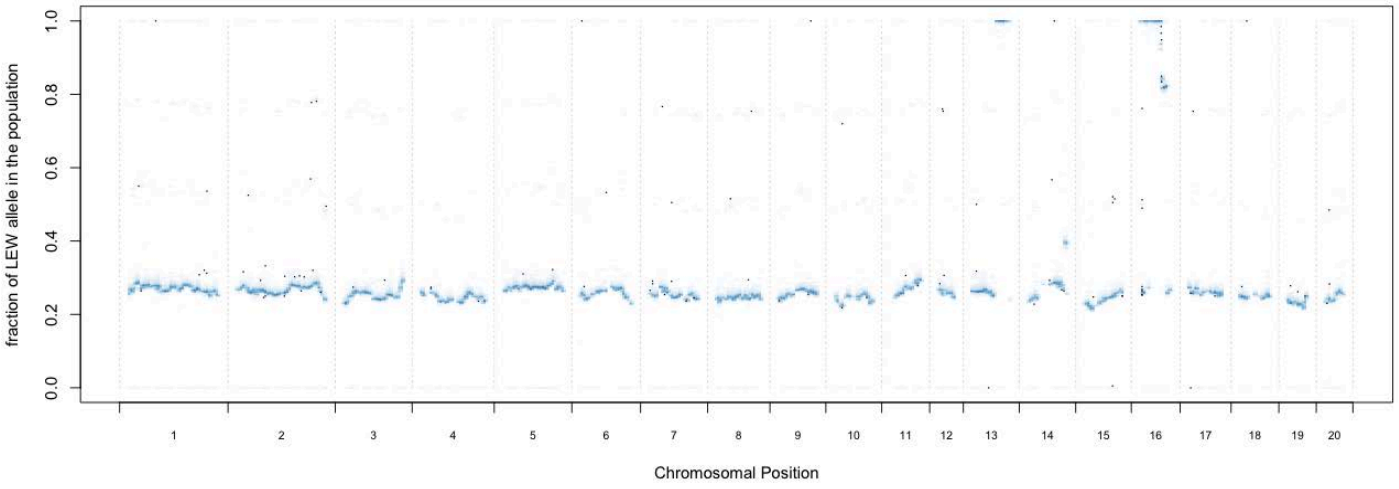
fraction of LEW allele in the population
0.0
0.2
0.4
0.6
0.8
1.0
1
2
3
4
5
6
7
8
9
10
11
12
13
14
15
16
17
18
19
20
Chromosomal Position

E

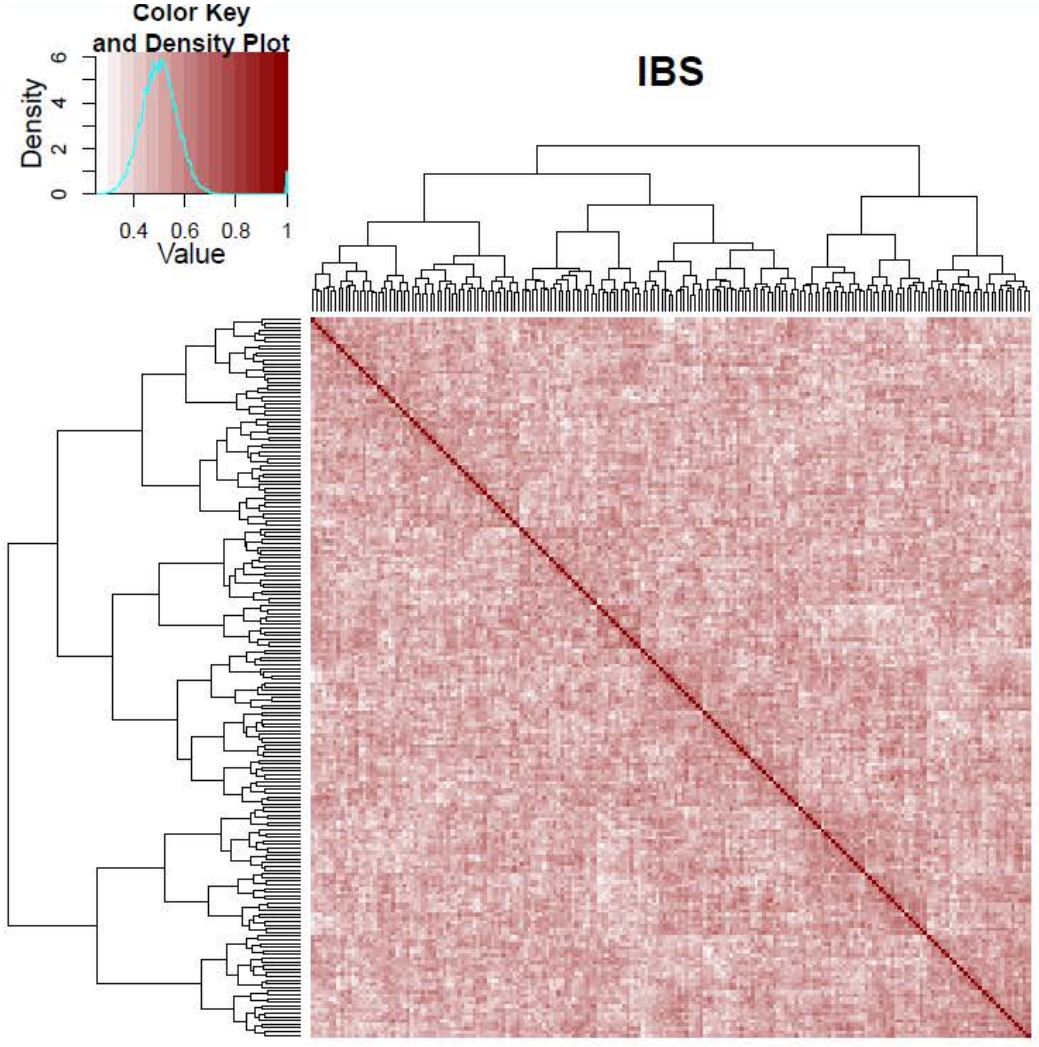
Color Key
and Density Plot
Density
0
2
4
6
0.4
0.6
0.8
1
Value
IBS

Figure S2. Related to Figure 1. eQTL analysis in the BMDMs derived from 200 back-cross rats. (**A**) Boxplots of expression data before and after normalization. Boxplots of log2-transformed expression data before (left panel) and after (right panel) RMA normalization, respectively. Each boxplot corresponds to one sample. Samples are shown in processing order. (**B**) Position of individual BC rats on first two principal components (PC) of the genome-wide expression data, before (left panel) and after (right panel) batch-effect corrections. Each rat is designated by a number corresponding to the batch it was processed. Parental congenic rats were culled and processed together with the rest of the BC rats controls (one for each batch) and they are shown in red. (**C**) Imputation of the missing genotypes in the BC population (n=200). All three panels represent a fraction of chromosome 20 genotype data in BC rats, where each row represents a SNP and each column represents an individual BC rat. Blue and red cells represent homozygous WKY-WKY and WKY-LEW heterozygous genotypes respectively, whereas white cells indicate missing genotypes. Genotyping data before (left panel) and after imputation (right panel) are shown. Genotyping errors were corrected in the lower panel. Imputation fills each missing value with the most likely genotype according to surrounding haplotype whereas genotype correction replaces isolated genotype calls according to their haplotypic context. (**D**) Average fraction of Lewis DNA in the population across the genome. 2D density plot of LEW allele frequency in the BC population according to genomic position, based on the 278,124 SNPs where the WKY genome differs from LEW. For the largest majority of SNPs, the frequency of LEW allele is close to 25%, consistent with the chosen back-cross strategy. SNPs where the frequency differs significantly from 0.25 reflect either congenics regions (see Methods), or failure of the genotype calling algorithm (isolated dots). All these SNPs were not taken into account for the eQTL analysis. (**E**) Heatmap of Identity by Sharing (IBS) in the WKY x LEW back-cross population. The normal distribution of IBS around 0.5 is consistent with the distribution expected under the absence of population structure.

.

Figure S3

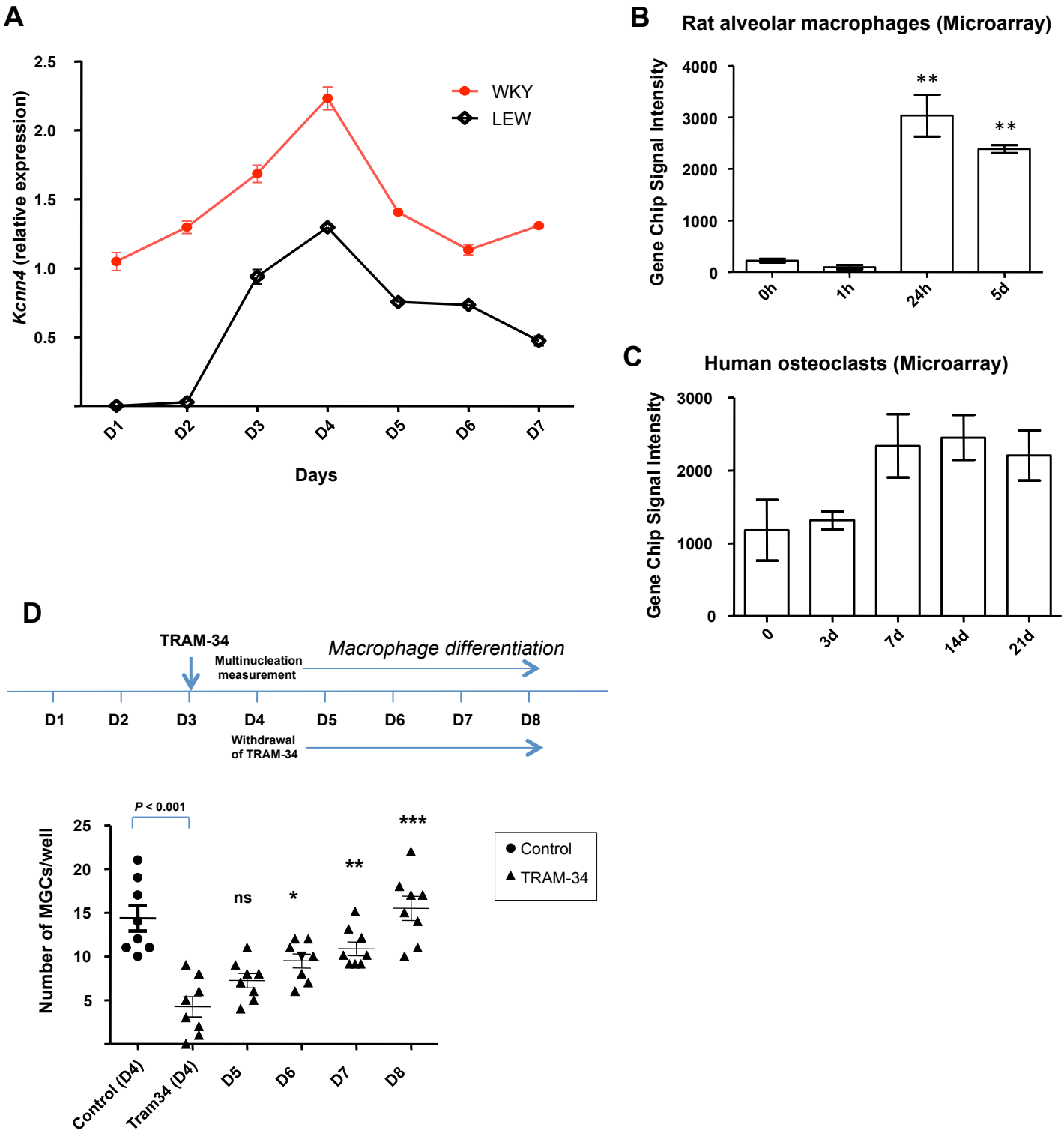

E

Differentiation (days)	D2	D3	D4	D5	D6	D7	D8
% of CD68+ cells (Control)	98	98	99	100	98	97	100
% of CD68+ cells (TRAM34)	99	100	97	100	100	98	99

F

Figure S3

Log(FC)	*P*-value	FDR	Gene symbol
-1.23	1.45×10^{-71}	2.17×10^{-67}	*Abcg1*
-1.71	2.82×10^{-71}	2.17×10^{-67}	*Serpinb2*
-1.34	2.17×10^{-57}	1.12×10^{-53}	*Scd*
-1.00	1.60×10^{-54}	6.19×10^{-51}	*Abca1*
-1.38	1.25×10^{-51}	3.86×10^{-48}	*Alpk2*
-0.92	5.57×10^{-45}	1.43×10^{-41}	*Irg1*
-0.80	1.27×10^{-43}	2.79×10^{-40}	*Slamf6*
-1.28	4.31×10^{-42}	8.32×10^{-39}	*P97600_RAT*
-1.10	5.36×10^{-42}	9.18×10^{-39}	*Marcksl1*
-1.17	6.24×10^{-42}	9.63×10^{-39}	*Olr1*
-1.31	2.91×10^{-39}	4.08×10^{-36}	*E9PSM5_RAT*
-1.22	8.49×10^{-39}	1.09×10^{-35}	*Mfng*
-0.91	1.09×10^{-38}	1.29×10^{-35}	*Cd8a*
-2.47	4.61×10^{-38}	5.08×10^{-35}	*LOC689963*
-1.33	2.35×10^{-33}	2.42×10^{-30}	*Kit*
-1.02	4.74×10^{-32}	4.57×10^{-29}	*Nrxn2*
-2.46	1.94×10^{-31}	1.76×10^{-28}	*Ccl6*
-1.58	2.67×10^{-30}	2.29×10^{-27}	*Mylip*
-0.62	1.86×10^{-29}	1.51×10^{-26}	*Malt1*
-0.88	3.38×10^{-28}	2.61×10^{-25}	*Atp2b4*

G

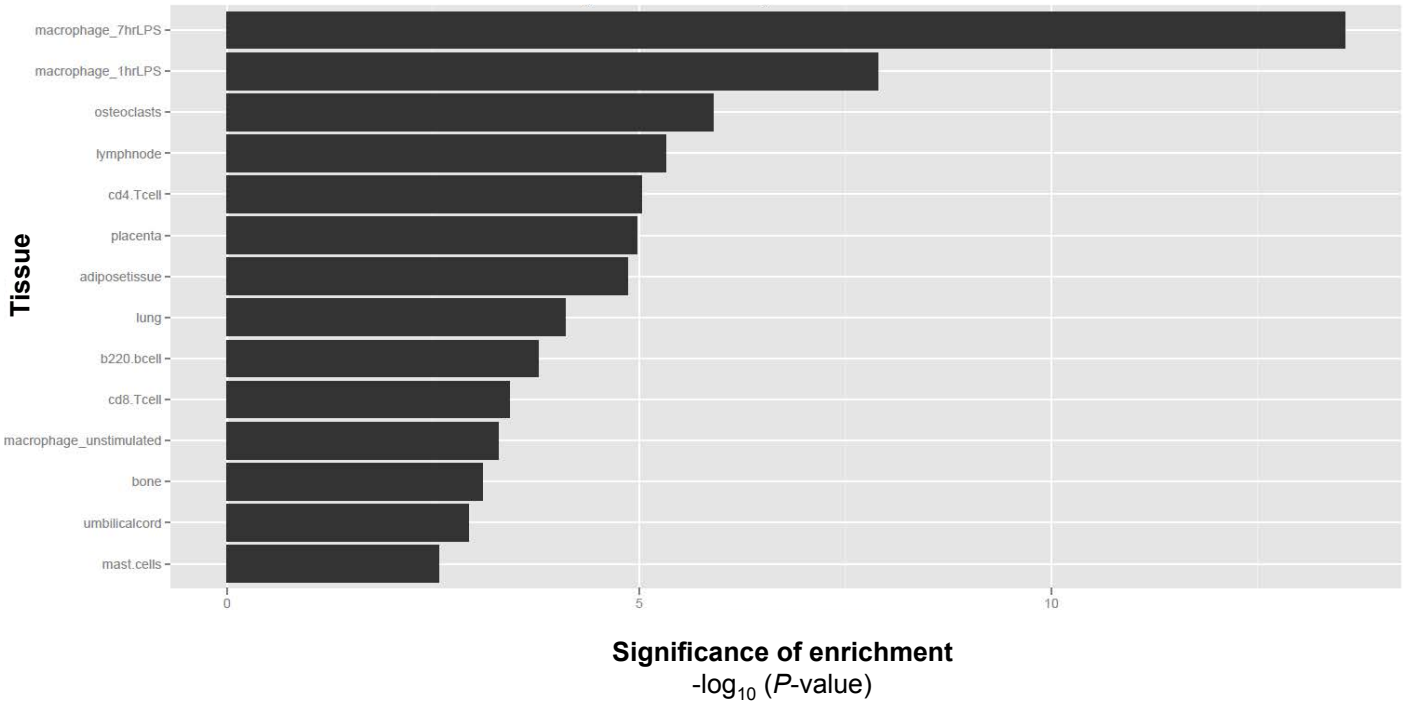

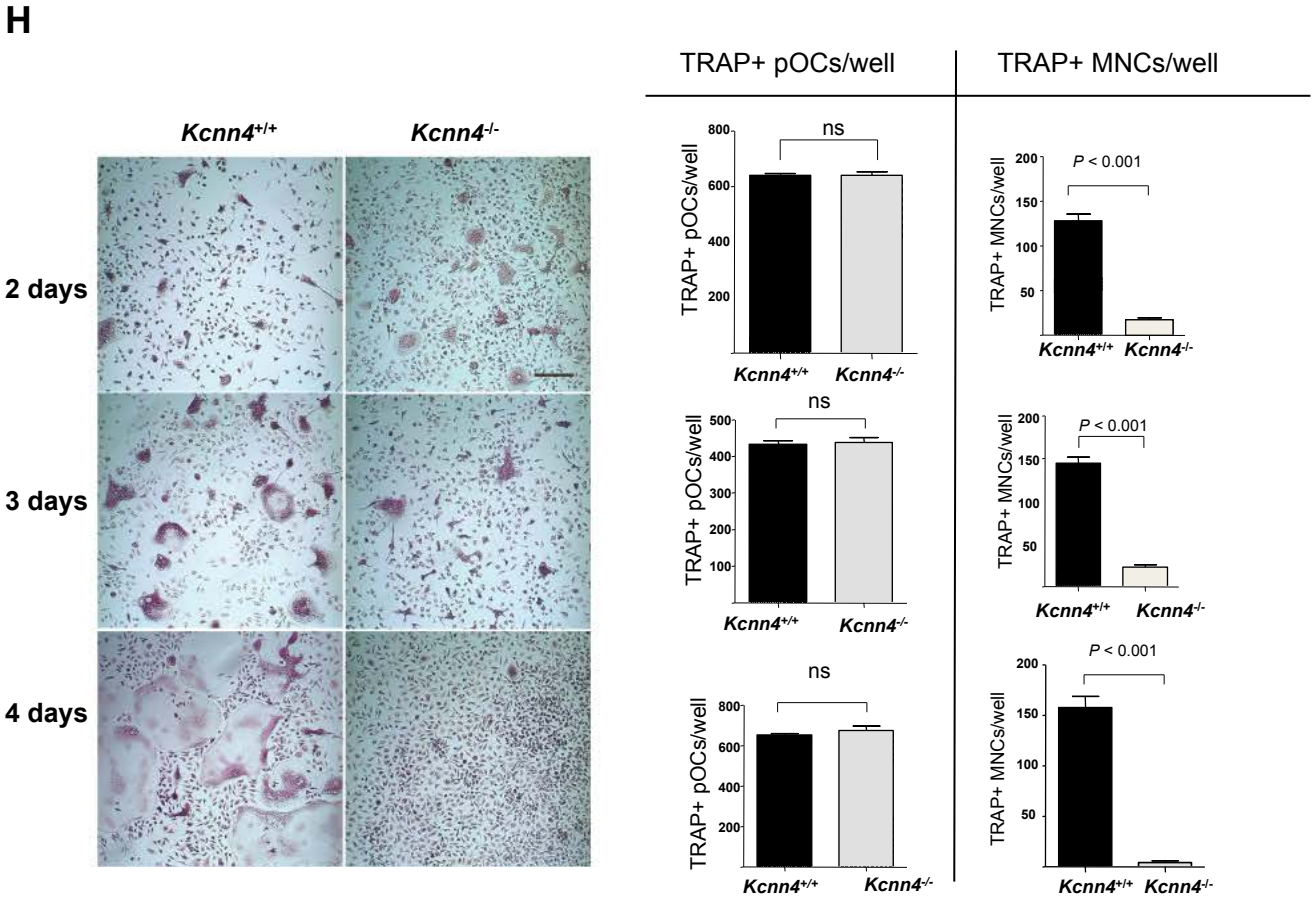

Figure S3. **Related to Figure 3**. *Kcnn4* expression is induced at the onset of macrophage fusion; Kcnn4 blockade is reversible and its genetic deletion does not affect pre-osteoclast formation. (**A**) Total RNA was extracted at Day 1 until Day 7 to assess *Kcnn4* expression by qRT-PCR in progressively multinucleating WKY BMDMs. Note the peak of Kcnn4 expression at day 4 in both strains and the relative increase in the fusion-competent WKY BMDMs. Relative expression values were normalised to *Hprt* expression. Error bars indicate SEM. (**B**) Total RNA was isolated from fusing rat alveolar macrophages (n=4) and subjected to Affymetrix Genechip analysis at different time points (0h, 1h, 24h, 5 days). Mean signal probe-set intensities are shown for rat *Kcnn4*. (**C**) Human monocyte-derived macrophages were cultured in the presence of M-CSF (20 ng/ml) and RANKL (10 ng/ml) for the indicated times to induce osteoclast differentiation and subjected to Affymetrix Genechip analysis. Mean signal probe-set intensities are shown for human *Kcnn4*. **, $P < 0.001$ when compared to 0h; error bars indicate SEM.

Figure S3. Related to Figure 3. (**D**) Bone marrow-derived macrophages from WKY rats were cultured at indicated times and incubated with TRAM-34 (10 μM) at day 3 (D3) where multinucleation occurs. TRAM-34 was then withdrawn from the culture media and the number of MGCs/well were determined as the number of cells containing > 10 nuclei at day 4 onwards. The lower panel shows the quantification of MGCs from D4. ns, non significant; *, $P < 0.05$; **, $P < 0.01$; ***, $P < 0.001$ when compared with TRAM-34 (D4). (**E**) % of CD68+ cells quantified by counting ED-1+ (rat CD68) cells during macrophage differentiation in control and media supplemented with TRAM-34. (**F**) RNA-seq analysis following selective pharmacological blockade of Kcnn4. The table shows the top 20 differentially expressed genes between WKY BMDMs treated with TRAM-34 (10 μM) when compared with untreated ones. FDR, False Discovery Rate; FC, fold change. (**G)** Tissue enrichment analysis of all the differentially expressed genes between control and TRAM-34 treated cells. (**H**) Bone marrow-derived macrophages from 6-week old *Kcnn4*$^{+/+}$ and *Kcnn4*$^{-/-}$ mice were cultured in the presence of M-CSF (25 ng/ml) and RANKL (20 ng/ml) for 2, 3 and 4 days to induce the differentiation of osteoclasts (Bar =100 μm, left panel). TRAP+ mononuclear cells (pre-osteoclasts) were quantified at each day during differentiation and the number of TRAP+ pre-osteoclasts/well reported (TRAP + pOCs/well). When the fusion outcome was measured as the number of large TRAP+ multinucleated cells (TRAP+ MNCs/well), there was a marked reduction in these cells in *Kcnn4*$^{-/-}$ mice at all considered time points. ns, non-significant. Error bars indicate SEM.

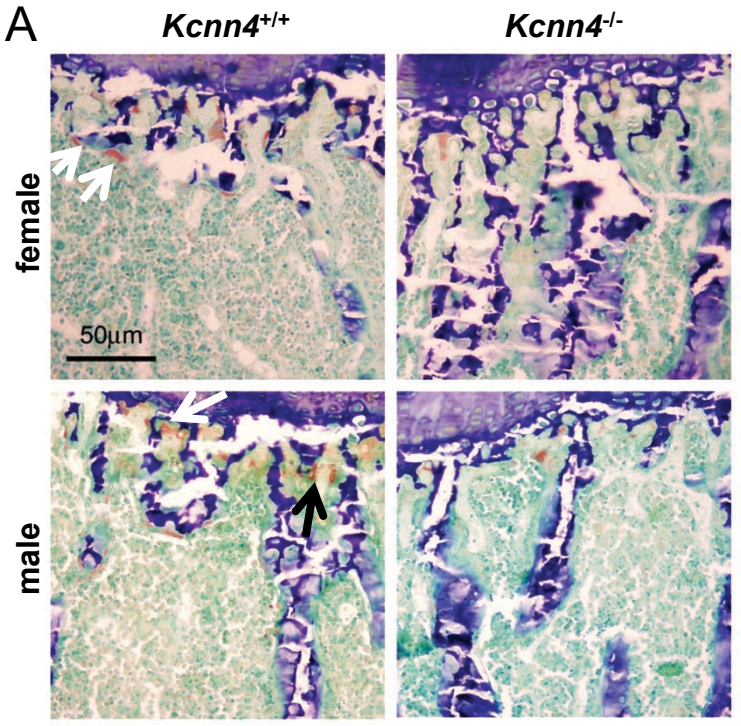
A
Kcnn4+/+
Kcnn4-/-
female
male
50µm

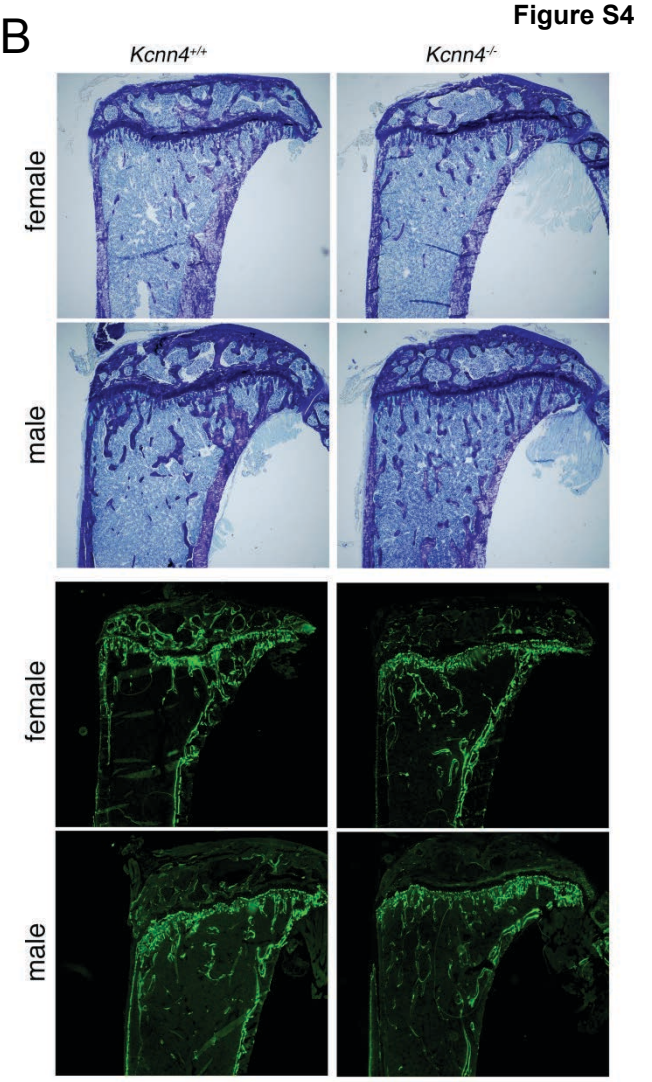
B
Kcnn4+/+
Kcnn4-/-
female
male
female
male

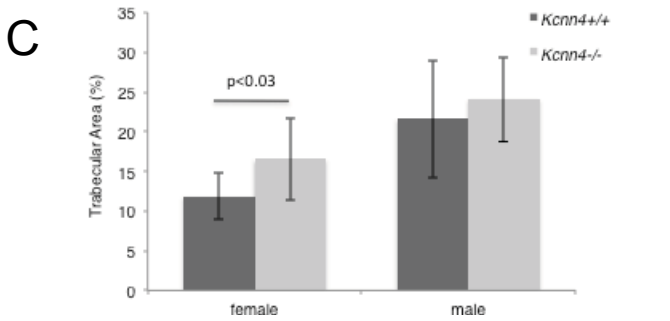
C
Kcnn4+/+
Kcnn4-/-
p<0.03
Trabecular Area (%)
female
male

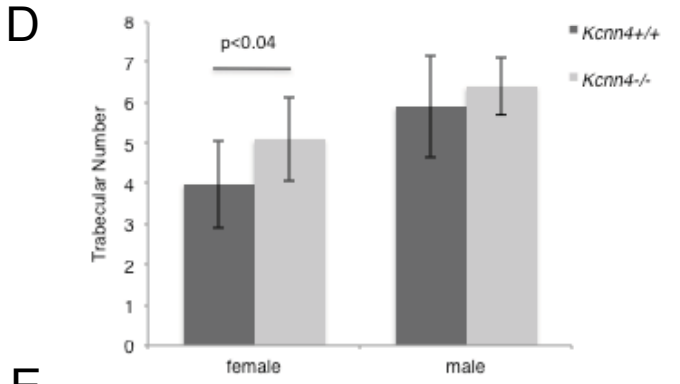
D
Kcnn4+/+
Kcnn4-/-
p<0.04
Trabecular Number
female
male

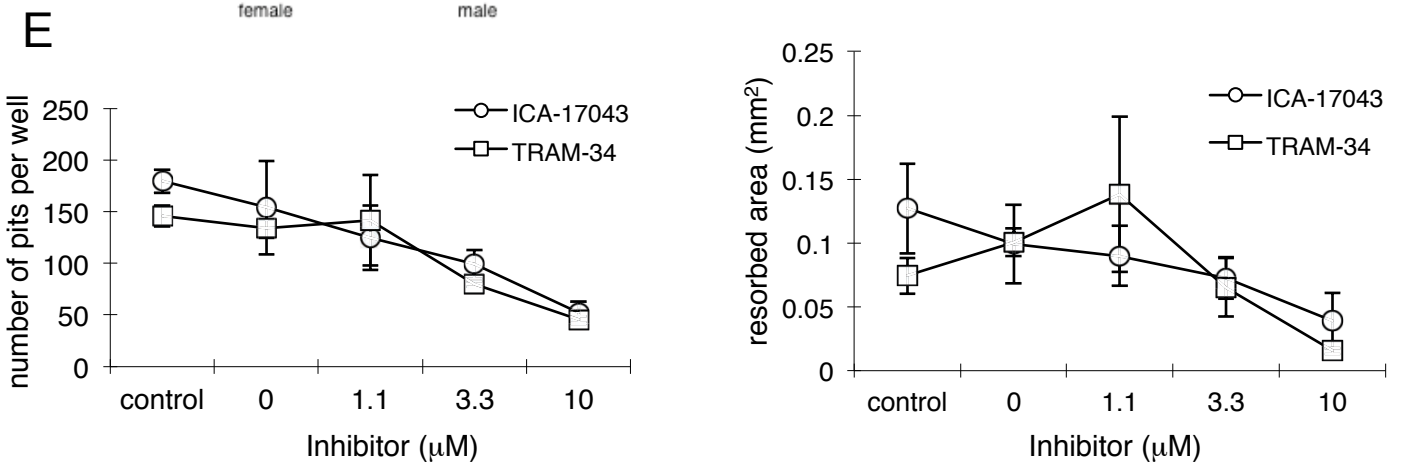
E
ICA-17043
TRAM-34
number of pits per well
control
0
1.1
3.3
10
Inhibitor (µM)
resorbed area (mm2)
ICA-17043
TRAM-34
control
0
1.1
3.3
10
Inhibitor (µM)

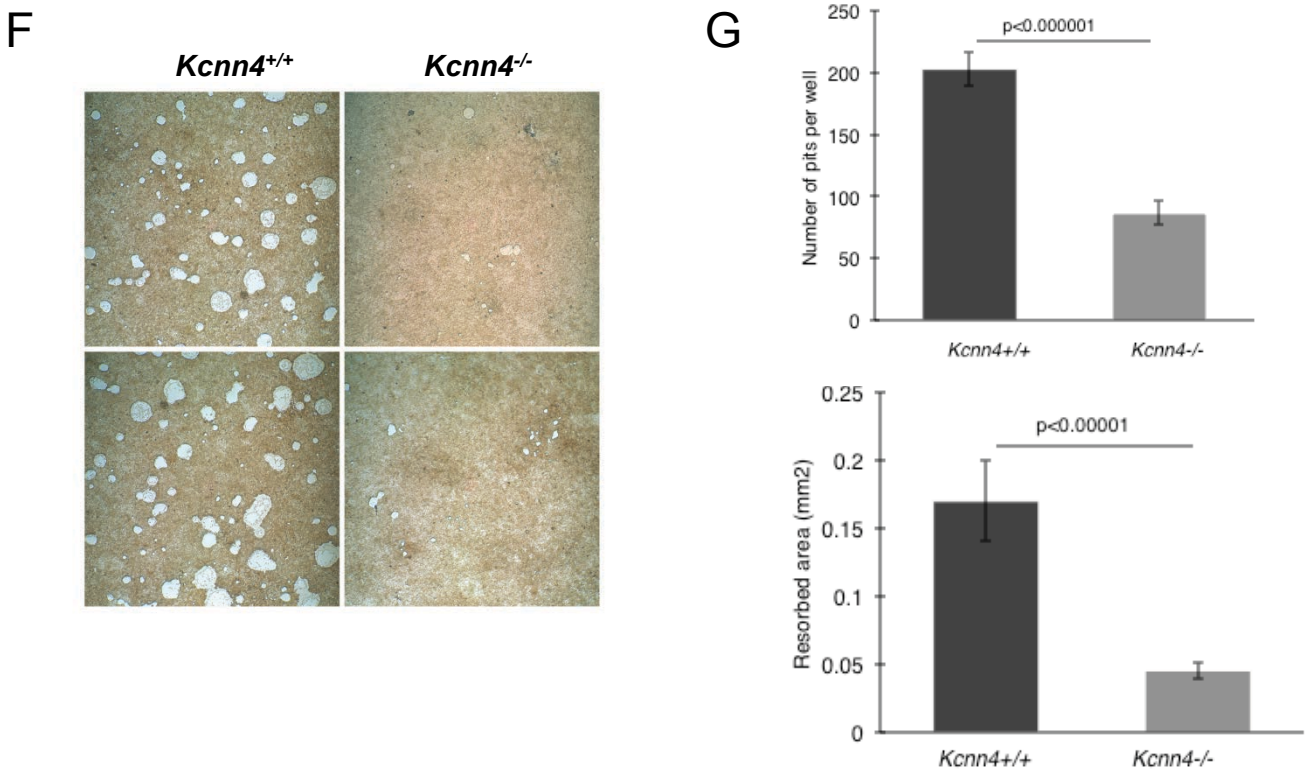

Figure S4. Related to Figure 4. *Kcnn4* affects osteoclast formation and activity. (**A**) Representative TRAP staining images of proximal tibiae from 8-week old *Kcnn4*$^{+/+}$ and *Kcnn4*$^{-/-}$ female and male mice. Note the reduced TRAP+ osteoclasts (in red) in male and female *Kcnn4*$^{-/-}$ mice tibiae. Arrows show the TRAP+ red staining in *Kcnn4*$^{+/+}$ mice. Original bar = 50μm. (**B**) Representative images of tibial bone sections for histomorphometry (static, upper two panels; dynamic, lower two panels; 8-week-old *Kcnn4*$^{+/+}$ and *Kcnn4*$^{-/-}$ female and male mice). (**C-D**) Histomorphometry analysis of Trabecular Area (**C**) and Trabecular Number (**D**). Data are reported as mean±SD (n=10 mice). (**E**) Mouse bone-marrow-derived macrophages were cultured in the presence of M-CSF (20 ng/ml) and RANKL (40 ng/ml) on calcium phosphate substrate coated chambers and treated with Kcnn4 inhibitors, TRAM-34 or ICA-17043. Graphs show quantitation data for the number of resorption pits per well (left panel) and the resorbed area per well (right panel). Error bars indicate SD. (**F**, **G**) Bone-marrow-derived macrophages from *Kcnn4*$^{+/+}$ and *Kcnn4*$^{-/-}$ mice were cultured in the presence of M-CSF (20 ng/ml) and RANKL (40 ng/ml) on calcium phosphate substrate coated chambers. (**F**) Representative images displaying resorption pits by osteoclasts. (**G**) Quantitation data for the number of resorption pits (upper) and the resorbed area per well (lower). Error bars indicate SD.

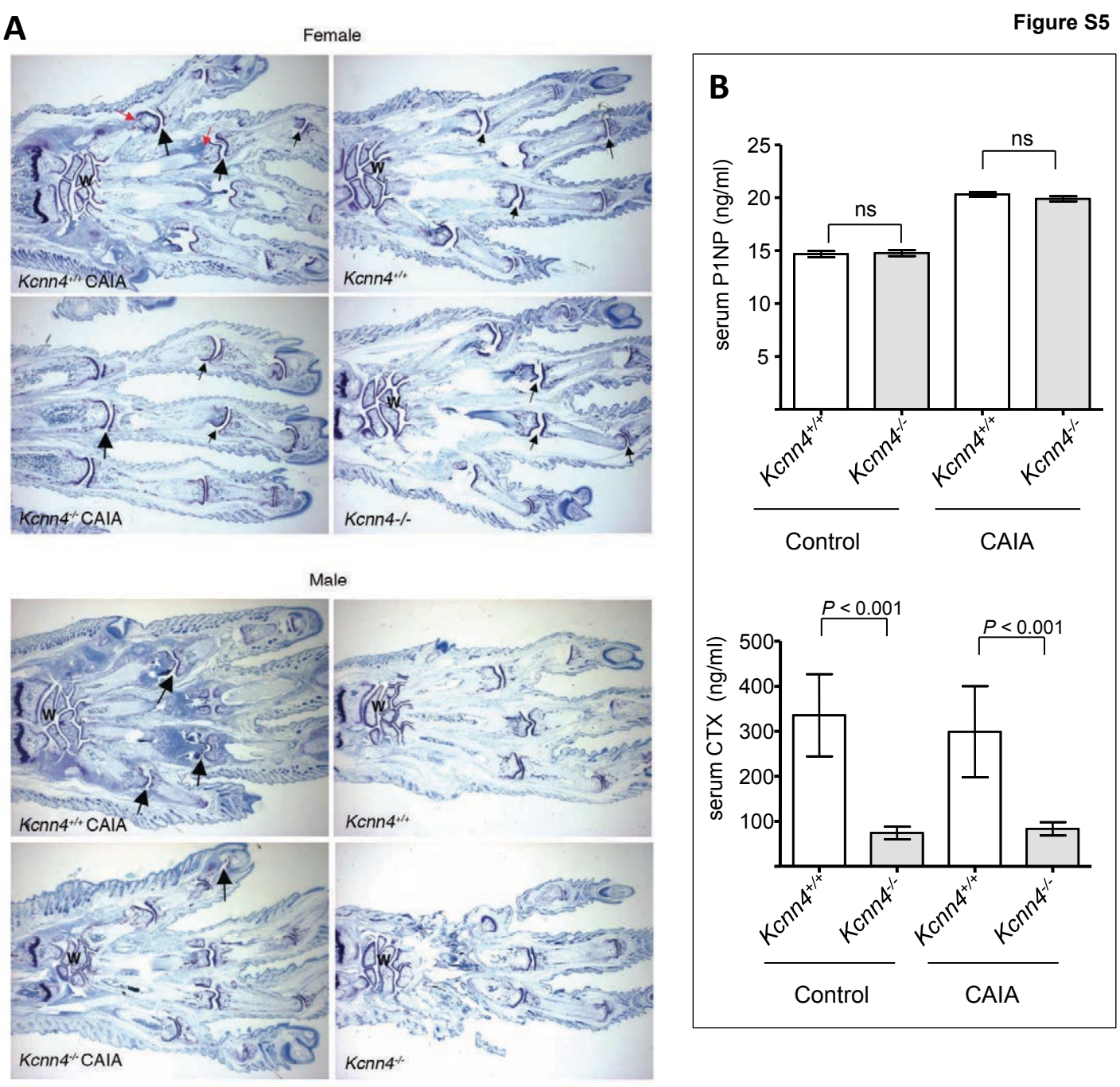

Figure S5. **Related to Figure S5**. Deletion of *Kcnn4* reduces anti-collagen antibody-induced bone erosion in chronic inflammatory arthritis. (**A**) Representative micrographs of the fore paws from *Kcnn4*$^{+/+}$ and *Kcnn4*$^{-/-}$ female (upper panel) and male (lower panel) naïve and CAIA-induced mice. Small arrows point out representative normal joints. Red arrows point out areas of subchondral bone resorption. W = wrist. Note the severe inflammation and cartilage damage with moderate pannus and bone resorption in joints of CAIA-induced *Kcnn4*$^{+/+}$ mice. This is in contrast with naïve and CAIA-induced *Kcnn4*$^{-/-}$ mice, which show no and minimal inflammation and cartilage damage, respectively. (**B**) Measurement of serum markers of bone formation (P1NP) and bone resorption (CTX) in control (naïve) and following CAIA induction in *Kcnn4*$^{+/+}$ and *Kcnn4*$^{-/-}$ animals. At least n=8 mice were used in each group. Error bars indicate SEM.

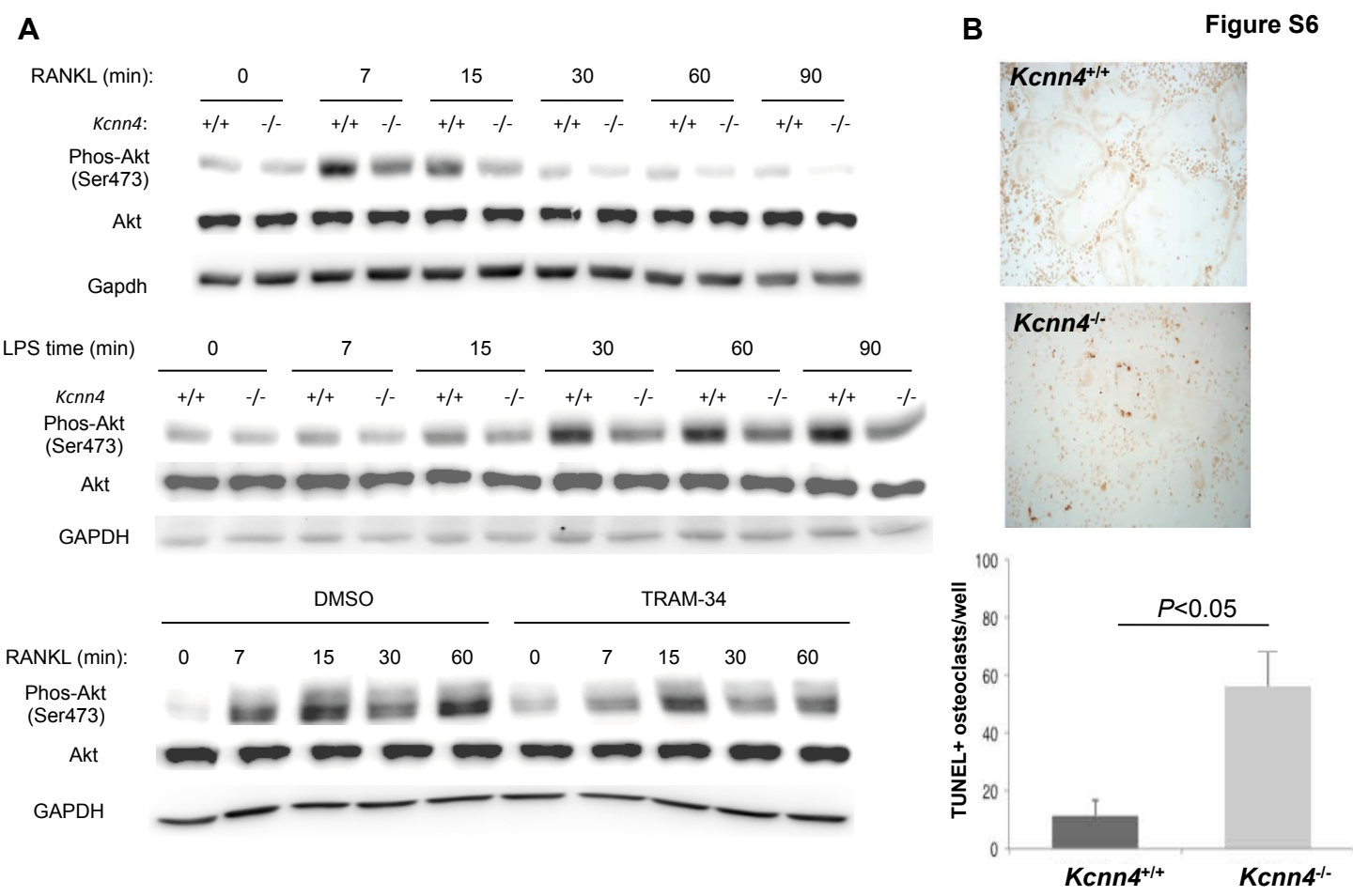

Figure S6. **Related to Figure 6**. AKT activation in the absence of *Kcnn4* in macrophages and the effect of *Kcnn4* deficiency on apoptosis in osteoclasts. (**A**) Western Blot analysis of BMDMs isolated from *Kcnn4*$^{+/+}$ and *Kcnn4*$^{-/-}$ mice were cultured in the presence of M-CSF (25 ng/ml) and RANKL (40 ng/ml) for 4 days, then cultured in the presence of M-CSF alone, with or without RANKL (40 ng/ml) or LPS (100 ng/ml) for the indicated times. Note the decrease in Akt (Ser473) phosphorylation in *Kcnn4*$^{-/-}$ macrophages treated with RANKL when compared with *Kcnn4*$^{+/+}$. Human monocyte-derived macrophages were pre-treated with TRAM-34 (10 mM) for 40 minutes and then stimulated with RANKL (100 ng/ml) for the indicated times. Similarly TRAM-34 prevented activation of Akt in human osteoclasts. These experiments were repeated 3 times with similar results and representative blots are shown. (**B**) Bone marrow derived macrophages from *Kcnn4*$^{+/+}$ and *Kcnn4*$^{-/-}$ mice were cultured in presence of M-CSF (25ng/ml) and RANKL (10ng/ml) for 4 days to induce the differentiation of osteoclasts. Cell were then incubated in serum and ligand (M-CSF/RANKL)-free media for 12 hours to induce apoptosis. TUNEL positive (dark brown colour) is observed in the nuclei of multinucleated osteoclasts that are undergoing apoptosis (upper panel). Following quantification, osteoclasts from *Kcnn4*$^{-/-}$ mice contained significantly more TUNEL-positive nuclei when compared to osteoclasts from *Kcnn4*$^{+/+}$ mice (lower panel). Error bars indicate SD.

Table S1. Related to Figure 4. Histomorphometric analysis of proximal tibiae from *Kcnn4*$^{+/+}$ and *Kcnn4*$^{-/-}$ mice. See extended protocols for the detailed description of all parameters.

parameters	Noc/BPm	Oc.Pm/BPm	Nob/TbPm	Ob.Pm/TbPm	O.Pm/Tb.pm	O.Ar/Tb.Ar	%Tb.Ar	Tb.Wi	Tb.N	Tb.Sp	L.Pm	%L.Pm	BFR/BV	BFR/TV	BFR/BS	MAR
	females															
	Kcnn4$^{+/+}$															
mean (sd)	2.19 (0.61)	0.43 (0.01)	4.05 (2.93)	0.04 (0.03)	0.09 (0.08)	0.06 (0.12)	11.86 (2.98)	30.30 (6.38)	3.98 (1.08)	239.0 (75.83)	0.47 (0.24)	9.83 (3.89)	262.23 (150.85)	33.81 (19.35)	13.14 (8.06)	1.26 (0.39)
	Kcnn4$^{-/-}$															
mean (sd)	0.95 (0.46)	0.012 (0.01)	3.30 (2.14)	0.03 (0.02)	0.06 (0.03)	0.01 (0.01)	16.54 (5.19)	31.83 (4.91)	5.08 (1.04)	173.48 (53.61)	1.22 (0.47)	21.68 (7.15)	754.43 (273.38)	122.38 (54.21)	39.44 (16.16)	1.82 (0.34)
t-test (p value)	0.0003	0.0008					0.04		0.04		0.0007	0.0006	0.0005	0.0004	0.0006	0.007
	males															
	Kcnn4$^{+/+}$															
mean (sd)	1.48 (0.41)	0.03 (0.01)	1.80 (0.93)	0.02 (0.01)	0.04 (0.02)	0.01 (0.01)	21.61 (7.39)	35.80 (6.95)	5.89 (1.26)	142.28 (48.99)	0.94 (0.30)	13.41 (5.72)	316.35 (167.31)	72.59 (33.02)	21.95 (12.40)	1.578 (0.43)
	Kcnn4$^{-/-}$															
mean (sd)	0.52 (0.23)	0.01 (0.01)	1.25 (0.71)	0.01 (0.01)	0.04 (0.03)	0.01 (0.01)	24.05 (5.30)	37.32 (5.56)	6.40 (0.70)	120.65 (20.85)	1.24 (0.36)	15.88 (5.49)	470.40 (196.41)	109.86 (42.79)	28.65 (11.80)	1.77 (0.34)
t-test (p value)	2.1E-05	2.2E-06												0.05		

Extended experimental procedures

Reagents

Rabbit polyclonal antibodies directed against p-38, phosphorylated-p38 (Thr180/Tyr182), p42/44MAPK , phosphorylated -p42/44MAPK (Thr202/Tyr204), Akt, phosphorylated –Akt (Ser473), CREB, phosphorylated -CREB (Ser133) were obtained from Cell Signaling Technology (Beverly, MA). A rabbit polyclonal antibody directed against the intracellular domain of MFR was published previously (Han et al., 2000). A rabbit polyclonal antibody directed against c-Fos, and a mouse monoclonal antibody directed against NFATc1 were purchased from Santa Cruz (Santa Cruz, CA). Rat monoclonal antibodies directed against mouse CD200 and CD44 were purchased from AbD Serotec (Kidlington, UK) and BD Biosciences (San Diego, CA), respectively. Mouse anti-GAPDH was purchased from Ambion (Austin, Texas). Horseradish peroxidase-conjugated F(ab')2 from goats directed against rabbit, rat and mouse IgG were purchased from Jackson ImmunoResearch (West Grove, PA). Phalloidin-Alexa fluor 568 and Tropo-3 was purchased from Invitrogen (Carlsbad, CA) and Osteologic slides from BD (Franklin Lakes, NJ). All supplies and reagents for tissue culture were endotoxin-free. Unless otherwise stated, all chemicals were from Sigma Chemical Co. (St Louis, MO). The Kcnn4 inhibitors, TRAM-34 and ICA-17043, were dissolved in 100% DMSO, and the final concentration of DMSO in culture was 0.1%, independent of the concentration of the inhibitors.

Genotype cleaning and imputation

The distribution of haplotype length shows a great overrepresentation of single SNP haplotypes. This overrepresentation can be attributed to genotyping errors that occur randomly in an independent manner. Thus isolated single SNP haplotype are likely to be caused by genotyping errors rather than true recombination events. Therefore, we reversed the genotype calling for all single SNP haplotype surrounded by 2 haplotypes of length

greater than 2 or for all cluster of several single SNP haplotype separated by one SNP each and surrounded by 2 haplotypes of length greater than 2. An example of the genotype Imputation and cleaning process can be seen of **Figure S2** (panel C)**.**

The WKY and LEW whole genome sequence data (Illumina HiSeq 2000; at least 10X coverage for both strains as described in (Atanur et al., 2013)) was then used to define the WKY and LEW allele at each individual SNP. SNPs where the WKY and LEW alleles could not be determined from the sequencing data were discarded resulting in 278,124 SNPs that can discriminate both alleles. Frequency of the WKY and LEW alleles across the whole genome can be seen in **Figure S2** (panel D). SNPs where the BRLMM clustering was not consistent with the breeding strategy (Heterozygous frequency < 0.35 or >0.65, presence of Lewis homozygous genotypes) were discarded leading to a final number of 242,252 SNPs. Missing genotypes were then imputed using fastPhase with the 2 founder haplotypes (**Figure S2**). The total number of SNPs for eQTL analysis were 1,974 following removal of those in complete linkage disequilibrium (r^2=1). The distribution of Identity by Sharing (IBS) was verified in all BC animals and confirmed the absence of any population structure (shown in **Figure S2**, panel E).

Primary macrophage, osteoclast cultures and assessment of cell multinucleation

Rat bone marrow derived macrophages (BMDMs) were cultured as previously described (Behmoaras et al., 2010). BMDMs were flushed from femur and tibia bones from rats and cultured in presence of L929-conditioned media for 4 days. To assess spontaneous MGC formation, macrophages were first dissociated using non enzymatic cell dissociation buffer (Sigma) and re-plated in Lab-Tek chambers (Fisher Scientific, UK). MGCs were then fixed at day 5 using Reastain Quick Diff and MGC quantification was performed by counting the number of nuclei in 100 macrophages using light microscopy. In some experiments TRAM-34 (10 μM, Tocris Biosceince, UK) was added to the cell culture during macrophage

differentiation to assess the effect of *Kcnn4* blockade on macrophage multinucleation and MGC formation. Bone marrow-derived osteoclasts were generated from four- to twelve-week old $Kcnn4^{+/+}$ and $Kcnn4^{-/-}$ mice as previously described (Cui et al., 2007). Bone marrow cells were isolated, mechanically dissociated and cultured at a density of 1.33 x 10^6 cells per cm^2 in a-MEM containing 10% heat inactivated FBS, 100 units/ml penicillin-streptomycin (Invitrogen, Carlsbad, CA), 1% MEM vitamins, 1 mM glutamine, and 5 to 30 ng/ml M-CSF (R&D, Minneapolis, MN). RANKL (R&D) was added at a concentration of 7 or 40 ng/ml. Culture medium was refreshed every three days. At the end of the culture, cells were fixed and reacted for tartrate-resistant acid phosphatase according to the supplier's directions. TRAP-positive cells with 3 nuclei or more were counted as osteoclasts as previously described (Li et al., 2005). Human monocyte derived macrophages were differentiated from buffy coats from healthy donors using gradient separation (Histopaque 1077, Sigma) and adhesion purification. Following Histopaque separation, peripheral blood mononuclear cells were re-suspended in RPMI (Life Technologies) and monocytes were purified by adherence for 1h at 37ºC, 5% CO_2. The monolayer was washed 6 times with HBSS to remove non-adherent cells and monocytes were matured for 5 days in RPMI containing 100 ng/ml M-CSF (PeproTech, UK). Macrophage purity was confirmed by immunohistochemical assessment of CD68 and > 99% cells were CD68+. In some experiments human peripheral blood monocytes were obtained from AllCells LLC (Emeryville, CA). Human osteoclasts were generated from normal peripheral blood monocytes or positively selected normal peripheral blood CD14+ cells (AllCells, Emeryville, CA). Peripheral blood monocytes were isolated using Ficoll-Paque and cultured at a concentration of 3 x 10^6 cells/ml in low glucose DMEM supplemented with 10% fetal bovine serum (FBS; Gemini Bio-Products, NC), recombinant human M-CSF (20 ng/ml) and recombinant human RANKL (10 ng/ml). The medium was refreshed twice a week. At the end of the culture, the cells were fixed and reacted for tartrate-

resistant acid phosphatase according to the supplier's directions. TRAP-positive cells with 3 nuclei or more were counted as osteoclasts.

eQTL analysis, network inference and cell type enrichment analysis

A transcript was designated as an eQTL when it mapped with a probability of 0.8 to a genomic region of less than 10 Mb. When multiple SNPs are located within the 10 Mb window, we referred to the SNP with the best marginal probability in that region as the associated SNP. We defined eQTL hotspots as SNPs linked to a significant over-representation of *trans* eQTLs by assuming that each of the 1071 *trans* eQTLs is associated at random to one of the 1974 haplotype tagging SNPs. The number of transcripts associated to a SNP follows a binomial distribution with parameters (1071, 1/1974). The Bonferroni-corrected 95% upper limit of the expected number of associated transcripts at each position, is then obtained by taking the α^{th} upper quantile of the distribution with α = 0.05/1974. A *trans* eQTL hotspot is defined by any SNP associated to more than 5 transcripts. eQTL hotspots located in the same LD block (r^2>0.8) were grouped and the *trans* cluster is defined as the whole set of transcripts mapping in *trans* to the LD block.

The network shown in Figure 1C was built by first extracting gene expression from the 184 genes of the network (190 transcripts) and adjusting the gene expression for the effect of *cis*-regulatory SNPs. R package *minet* was used to compute the mutual information between all pairs of gene as well as between all pair of genes and the chromosome 9 locus SNP, and ARACNE (Basso et al., 2005) was used to remove indirect edges from the network. Cell type enrichment analysis was performed using the Mouse GNF1M Gene Atlas data (GSE1133), containing expression from 78 tissues and cell types. Log transformed normalized expression was used and for each gene *g* and cell type *c*, a Z-score was computed to measure the relative overexpression of gene *g* in cell type *c* compared to other cell types. Each Z-score was then assigned a *P*-value for significance of the overexpression assuming normal distribution of the

Z-scores. Finally, for each cell type, enrichment of the network was computed by counting the number of genes with a significant *P*-values at a marginal 0.05 level, inside and outside of the network and using an hypergeometric test for enrichment.

LPS-induced calvarial bone resorption assay

To assess osteoclast formation and activity *in vivo*, we administered a single local subperiosteal calvarial injection of LPS (25 μg in 2 μl; Escherichia coli O55:B5, Sigma Chemical, St. Louis, MO) to 8-week-old male and female wild type and *Kcnn4*$^{-/-}$ mice that were sacrificed 5 days later. Because the angle of the needle is kept fixed during the injection, the osteoclast pits tend to remain in the vicinity of the injected site. Animals were checked daily for the five-day duration of the experiment, including weekends and holidays, when applicable. Those animals showing evidence of pain, were administered analgesics based on consultation with a veterinarian. Calvariae were subjected to microCT analysis, and resorbed areas were quantified using ImageJ software (NIH, Bethesda, MD). All procedures were approved by the Yale University Institutional Animal Care and Use Committee.

Measurement of bone turnover markers

Serum samples were obtained from *Kcnn4*$^{+/+}$ and *Kcnn4*$^{-/-}$ mice at sacrifice in control and following CAIA and were stored at −80 °C. N-terminal propeptide of type 1 procollagen (P1NP) and C-terminal cross-linked telopeptide of type I collagen (CTX) levels were determined by enzyme immunoassay using IDS kits AC-33F1 and AC-06F1, respectively (Immunodiagnostic Systems).

RNA-seq library preparation and data analysis in primary macrophages

Total RNA was extracted from WKY macrophages (+/- TRAM-34, 10μM) using Trizol (Invitrogen) according to manufacturer's instructions with an additional purification step by on-column DNase treatment using the RNase-free DNase Kit (Qiagen) to ensure elimination of any genomic DNA. The integrity and quantity of total RNA was determined using a

NanoDrop 1000 spectrophotometer (Thermo Fisher Scientific) and Agilent 2100 Bioanalyzer (Agilent Technologies). 1μg of total RNA was used to generate RNA-seq libraries using TruSeq RNA sample preparation kit (Illumina) according to the manufacturer's instructions. Briefly, RNA was purified and fragmented using poly-T oligo-attached magnetic beads using two rounds of purification followed by the first and second cDNA strand synthesis. Next, cDNA 3' ends were adenylated and adapters ligated followed by 10 cycles of library amplification. Finally, the libraries were size selected using AMPue XP Beads (Becmkan Coulter) purified and their quality was checked using Agilent 2100 Bioanalyzer. Samples were randomized to avoid batch effects and libraries were run on a single lane per sample of the HiSeq 2000 platform (Illumina) to generate 75bp paired-end reads. RNA-seq reads were then aligned to the rn4 reference genome using tophat 2 and non-uniquely aligned reads where discarded leading to coverage of ~40M reads and 35M uniquely mapped reads. Gene level read counts were computed using HT-Seq and genes with less that 10 aligned reads across all samples were discarded prior to analysis leading to 15,155 genes. Differential expression analyses between the two groups were carried out using edgeR and using a 5% FDR to call significant differentially expressed genes. Cell type enrichment analysis was performed using the Mouse GNF1M Gene Atlas data (GSE1133), containing expression from 78 tissues and cell types. Log transformed normalized expression was used and for each gene *g* and cell type *c*, a Z-score was computed to measure the relative overexpression of gene *g* in cell type *c* compared to other cell types. Each Z-score was then assigned a *P*-value for significance of the over-expression assuming normal distribution of the Z-scores. For each cell type, enrichment of the set of differentially expressed genes was computed by counting the number of genes with significant *P*-values at a marginal 0.05 level, inside and outside of the set of differentially expressed genes and using an hypergeometric test for enrichment.

siRNA and qRT-PCR

On day 5 of culture, WKY BMDMs were replated in six-well plates ($1x10^6$ cells per well) in DMEM (Invitrogen) overnight and transfected for 48 hours with siGENOME SMARTpool for either human or rat *Trem2*, and rat *Treml1*, Trem1, *D3ZDX3_Rat* (100 nM, Dharmacon) or siGENOME non-targeting siRNA pool as the scrambled control siRNA using Dharmafect 1 (1:50, Dharmacon) as a transfection reagent in OPTIMEM medium (Invitrogen). For human monocytes-derived macrophages (MDMs), cells were incubated on day 5 of cluture with either human *TREM2* siRNA or siGENOME non-targeting siRNA pool. The siRNA sequences used in the siGENOME SMARTpool for all transcripts are available upon request. All qRT-PCRs were performed with an ABI 7900 Sequence Detection System (Applied Biosystems, Warrington, UK). A two-step protocol was used beginning with cDNA synthesis with iScript select (Bio-Rad) followed by PCR using SYBR Green Jumpstart Taq Ready Mix (Sigma). A total of 10ng of cDNA per sample was used. All samples were amplified using a set of 4 biological replicates with three technical replicates used per sample in the PCR analysis. Sequence detection software (SDS) version (Applied Biosystems) was used to obtain the Ct values. Results were analysed using the comparative Ct method and each sample was normalised to the reference gene *Hprt*, to account for any cDNA loading differences. The primer sequences are available upon request.

Histomorphometric analysis of the bone

Histomorphometry was performed 0.25 mm proximal to the growth plate using Osteomeasure software (Osteometrics, Atlanta, GA). The following parameters were measured: the relative tissue surface occupied by bone (B.Ar/T.Ar; %); the number of trabeculae per mm (Tb.N /mm); the relative surface of bone occupied by trabeculae (Tb.Ar; %); the distance/separation between trabeculae (μm); the number of osteoclasts per total bone surface (Oc/T.Ar); the perimeter of osteoclasts per total bone perimeter (Oc.Pm./B.Pm); the perimeter of osteoblasts

per total bone perimeter (Ob.Pm/B.Pm), mineralizing surface (MS/BS), mineral apposition rate (MAR), and bone formation rate (BFR/BV).

Scoring and histopathological evaluation of collagen antibody-induced arthritis (CAIA)

The scoring system for CAIA was 0 = normal; 1 = erythema and edema in 1-2 digits; 2 = erythema and edema in >2 digits or mild erythema and edema, usually in the ankle joint; 3 = moderate erythema and edema encompassing the tarsal joint; 4 = severe erythema and edema encompassing the tarsal and metatarsal joint. This analysis was completed by Bolder BioPath (Boulder, Co). Formalin fixed joints (right and left fore and hind paws, both ankles and both knees) were decalcified in 5% formic acid for 2-3 days; tissues were trimmed, processed for paraffin embedding, sectioned at 8 μm and stained with toluidine blue. Both hind paws, both fore paws, and both knees were embedded and sectioned in the frontal plane while ankles were sectioned in the sagittal plane or ankles may be sectioned with hind paws in the frontal plane. All sections were scored without knowledge of the treatment groups. Groups were later identified as follows. When scoring paws or ankles from mice with arthritic lesions, severity of changes as well as number of individual joints affected were recorded. When only 1-3 joints of the paws or ankles out of a possibility of numerous metacarpal/metatarsal/digit or tarsal/tibio-tarsal joints were affected, an arbitrary assignment of a maximum score of 1, 2 or 3 for parameters below was given depending on severity of changes. If more than 3 joints were involved, the criteria below were applied to the most severely affected/majority of joints. Inflammation: 0 = Normal; 1 = Minimal infiltration of inflammatory cells in synovium and periarticular tissue of affected joints; 2 = Mild infiltration of inflammatory cells. If referring to paws, generally restricted to affected joints (1-3 affected); 3 = Moderate infiltration with moderate edema. If referring to paws, restricted to affected joints, generally 3-4 joints + wrist or ankle; 4 = Marked infiltration affecting most areas with marked edema, 1 or 2 unaffected joints may be present; 5 = Severe diffuse infiltration with severe edema

affecting all joints and periarticular tissues. Pannus: 0 = Normal; 1 = Minimal infiltration of pannus in cartilage and subchondral bone, marginal zones; 2 = Mild infiltration with marginal zone destruction of hard tissue in affected joints; 3 = Moderate infiltration with moderate hard tissue destruction in affected joints; 4 = Marked infiltration with marked destruction of joint architecture, affecting most joints; 5 = Severe infiltration associated with total or near total destruction of joint architecture, affects all joints. Cartilage Damage: 0 = Normal; 1 = Minimal = generally minimal to mild loss of toluidine blue staining with no obvious chondrocyte loss or collagen disruption in affected joints; 2 = Mild = generally mild loss of toluidine blue staining with focal areas of chondrocyte loss and/or collagen disruption in some affected joints; 3 = Moderate = generally moderate loss of toluidine blue staining with multifocal chondrocyte loss and/or collagen disruption in affected joints, some matrix remains on any affected surface with areas of severe matrix loss; 4 = Marked = marked loss of toluidine blue staining with multifocal marked (depth to deep zone) chondrocyte loss and/or collagen disruption in most joints, if knee-one surface with total to near total cartilage loss; 5 = Severe = severe diffuse loss of toluidine blue staining with multifocal severe (depth to tide mark) chondrocyte loss and/or collagen disruption in all joints, if knee-2 or more surfaces with total to near total cartilage loss. Bone Resorption: 0 = Normal; 1 = Minimal = small areas of resorption, not readily apparent on low magnification, rare osteoclasts in affected joints, restricted to marginal zones; 2 = Mild = more numerous areas of resorption, not readily apparent on low magnification, osteoclasts more numerous in affected joints, restricted to marginal zones; 3 = Moderate = obvious resorption of medullary trabecular and cortical bone without full thickness defects in cortex, loss of some medullary trabeculae, lesion apparent on low magnification, osteoclasts more numerous in affected joints; 4 = Marked = full thickness defects in cortical bone, often with distortion of profile of remaining cortical surface, marked loss of medullary bone, numerous osteoclasts, affects most joints; 5

= Severe = full thickness defects in cortical bone and destruction of joint architecture of all joints. For each animal, the inflammation, pannus, cartilage damage and bone damage scores were determined for each of the 8 joints submitted. A sum total (all 8 joints) animal score and an eight joint mean animal score was determined as well as sums and means for each of the individual parameters. Parameters for the various groups were then compared with Group A (vehicle) using a Student's t-test or other appropriate analysis methods with significance set at $p \leq 0.05$.

Calcium oscillations and electrophysiology

Bone marrow-derived macrophages isolated from *Kcnn4*$^{+/+}$ and *Kcnn4*$^{-/-}$ mice were plated on 12-mm diameter coverglass that were placed in 24-well dishes. Cells were cultured in the presence of M-CSF (25 ng/ml) supplemented or not with RANKL (10 ng/ml). Oscillations were recorded 3 days later. Cells were incubated for 30 minutes at 30°C in loading solution (115 mM NaCl, 5.4 mM KCl, 1 mM MgCl2, 2 mM CaCl2, 20 mM HEPES, and 10 mM glucose, pH 7.42) supplemented with 5 μM Fura-2/AM (Invitrogen). Fura-2 fluorescent images were analyzed using an inverted microscope (ECLIPSE TE300, Nikon) and a video image analysis system (Argus-50/CA, Hamamatsu Photonics) with excitation filters at 340 ±10 and 380 ± 10 nm, a dichroic beam splitter at 400 nm, and a bandpass emission filter at 510–550 nm. The recording solution contained 115 mM NaCl, 5.4 mM KCl, 1 mM $MgCl_2$, 2 mM $CaCl_2$, 20 mM HEPES, and 10 mM glucose, pH 7.42. Data are presented as mean ± standard error of the mean (SEM) and statistical significance was determined using the Student's t-test.

Electrophysiology

For electrophysiology, macrophages plated on 12-mm diameter coverslips were transferred to a recording chamber and superfused (~1 ml/min) with external solution: 145 mM NaCl, 5 mM KCl, 2 mM CaCl2, 1 mM MgCl2, 10 mM HEPES, 2.5 mM Glucose, pH 7.4. Pipettes

had a resistance of 3-9 MΩ when filled with internal solution: 120 mM KCl, 2 mM MgCl2, 10 mM HEPES, 20 mM glucose, 10 mM EGTA, pH 7.3. To achieve a free internal Ca^{2+} concentration of 10^{-6} M in the presence of 10 mM EGTA, 8.98 mM CaCl2 was added to the internal solution (23). In some experiments, 1 μM ICA-1703 was included in the external solution. Experiments were performed using an upright microscope (Olympus BX51WI, Olympus, Center Valley, PA) under phase-contrast optics (60x objective, NA 0.9) and at room temperature. An Axopatch 200B patch clamp amplifier, Digidata 1322A digitizer, and PClamp9 software (Axon Instruments, CA) were used for recordings (2 kHz low-pass filtered; 5 kHz sampling rate). Cells were maintained at a holding potential of -60 mV. Voltage steps from -100 mV to + 80 mV (400 ms) and voltage ramps (-140 mV to +120 mV over 200 ms) were applied to generate current / voltage plots in Clampfit 9.0 (Axon Instruments, CA).

Immunohistochemistry and Immunofluorescence

For ED-1 (AbD Serotec, Oxford, UK) immunostaining, formalin-fixed, paraffin-embedded rat tissues were microwaved in sodium citrate buffer for antigen retrieval. Following consecutive blocking steps (peroxide block for 15 min, 10% goat serum block for 15 min, followed by a 10% milk block for 15 min), sections were incubated with the primary antibody ED-1 (1:500) and the slides left for 1 h at room temperature. The slides were then washed and incubated in the polymer-HRP (Dako mouse EnVision kit, Dako, Denmark) for 30 min at room temperature. Staining was visualized using DAB (Dako EnVision kit) and sections counterstained with hematoxylin, dehydrated, and mounted with cover slips. For visualization of the acting cytoskeleton and nuclei, cells were fixed in 4% paraformaldehyde (PFA) for 20 minutes at room temperature and stained with rhodamine-phalloidin (Molecular Probes, Eugene, OR, USA) and 4′,6-diamidino-2-phenylindole (DAPI; Sigma) as described (MacLauchlan et al., 2009).

Western Blotting

After four to seven days of culture, osteoclasts were serum-starved for three to four hours and stimulated with the indicated reagents. The cells were then lysed in Laemmli sample buffer supplemented with protease inhibitors (cOmpleteTM protease inhibitor tablets; Roche Molecular Biochemicals), sodium fluoride, and a phosphatase inhibitor cocktail II (Roche). The lysates were sonicated and resolved by SDS-PAGE, transferred to PVDF membranes, and subjected to immunoblotting with appropriate primary and secondary antibodies. The probed proteins were detected using SuperSignal West Femto Cheluminescent Substrate (Thermo Fisher Scientific Inc., Rockford, IL).

Statistical Analysis

Unless otherwise stated, data represent the mean ± one standard deviation (SD). Treatment groups were compared using the analysis of variance. Unless otherwise stated, pairwise comparison p-values between the treatment groups were adjusted using Tukey multiple comparison procedure. Statistical significance was declared if the two-sided *p*-value is < 0.05.

Supplemental References

Atanur, S.S., Diaz, A.G., Maratou, K., Sarkis, A., Rotival, M., Game, L., Tschannen, M.R., Kaisaki, P.J., Otto, G.W., Ma, M.C.*, et al.* (2013). Genome Sequencing Reveals Loci under Artificial Selection that Underlie Disease Phenotypes in the Laboratory Rat. Cell *154*, 691-703.

Basso, K., Margolin, A.A., Stolovitzky, G., Klein, U., Dalla-Favera, R., and Califano, A. (2005). Reverse engineering of regulatory networks in human B cells. Nat Genet *37*, 382-390.

Behmoaras, J., Smith, J., D'Souza, Z., Bhangal, G., Chawanasuntoropoj, R., Tam, F.W., Pusey, C.D., Aitman, T.J., and Cook, H.T. (2010). Genetic loci modulate macrophage activity and glomerular damage in experimental glomerulonephritis. Journal of the American Society of Nephrology : JASN *21*, 1136-1144.

Cui, W., Cuartas, E., Ke, J., Zhang, Q., Einarsson, H.B., Sedgwick, J.D., Li, J., and Vignery, A. (2007). CD200 and its receptor, CD200R, modulate bone mass via the differentiation of osteoclasts. Proc Natl Acad Sci U S A *104*, 14436-14441.

Han, X., Sterling, H., Chen, Y., Saginario, C., Brown, E.J., Frazier, W.A., Lindberg, F.P., and Vignery, A. (2000). CD47, a ligand for the macrophage fusion receptor, participates in macrophage multinucleation. J Biol Chem *275*, 37984-37992.

Li, H., Cuartas, E., Cui, W., Choi, Y., Crawford, T.D., Ke, H.Z., Kobayashi, K.S., Flavell, R.A., and Vignery, A. (2005). IL-1 receptor-associated kinase M is a central regulator of osteoclast differentiation and activation. J Exp Med *201*, 1169-1177.

MacLauchlan, S., Skokos, E.A., Meznarich, N., Zhu, D.H., Raoof, S., Shipley, J.M., Senior, R.M., Bornstein, P., and Kyriakides, T.R. (2009). Macrophage fusion, giant cell formation, and the foreign body response require matrix metalloproteinase 9. Journal of leukocyte biology *85*, 617-626.